XXV AIAS NATIONAL CONFERENCE
INTERNATIONAL CONFERENCE ON MATERIAL ENGINEERING
Gallipoli - Lecce, 4-7 September 1996

A FIRST GENERATION X-RAY MICROTOMOGRAPHY SYSTEM FOR NON-DESTRUCTIVE MATERIALS TESTING

F. Bertolino*, G. Gatto*, F. Ginesu*, P. Randaccio**

* Department of Mechanical Engineering,
University of Cagliari
Piazza d'Armi, 09123 ITALY

**Department of Physics
University of Cagliari
Via della Pineta, 09123 ITALY

KEYWORDS: Tomography, non-destructive testing

ABSTRACT

The purpose of this paper is to describe the prototype of a first generation X-ray microtomograph for the non-destructive testing of mechanical components. Following a brief presentation of the system, characterisation tests, the purpose of which is to highlight the system's limits and sphere of applicability, are discussed. Some significant results are then illustrated.

INTRODUCTION

Today, many investigative techniques for non-destructive materials testing are available. These range from classic strain tests to photoelasticity and from holographic and moiré interferometry to the use of ultrasounds and X-rays [1-4]. Each technique has its own characteristic field of application, accuracy, times and modalities. These techniques, however, rarely afford the possibility of locating with precision damage within the volume and it is therefore important to develop testing methods using tomography (from the Greek *tomos* meaning section). Computerised X-ray Tomography (CT) consists of the reconstruction of a succession of cross-sections of the object under examination starting from X-ray pictures taken from different angles [5-6]. CT can be applied whenever an object is submitted to any form of energy which propagates inside it following known trajectories, usually straight lines. For example, with interferometric tomography it is possible to study variations in the refractive index inside a semi-transparent object, such as Pyrex [7] or a fluid [8]. By means of X-ray tomography it is possible to analyse different kinds of materials (metals, plastics, ceramics, composites) or check the assembly of a complex piece.

The authors have developed an X-ray microtomography system that allows the study of objects of small dimensions. In the course of the report, following the description of the system, the results of characterisation tests are presented.

DESCRIPTION OF THE TOMOGRAPH

An X-ray system (HP FAXITRON model 43855A) suitable for X-raying small objects (contained within an ideal sphere with a radius of 20 cm) was equipped with the instruments necessary to create the prototype of a first generation X-ray microtomography system (Fig. 1). The X-rays travel inside a lead chamber from top to bottom: the point detector is positioned at the base, roughly 80 cm from the source. It converts the rays transmitted through the object into an electronic signal that can be processed automatically. The test pieces are arranged cantilever-wise on a handling system and this limits their weight.

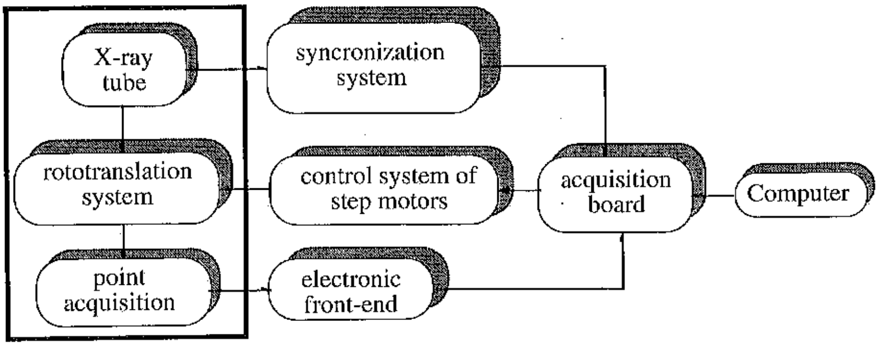

Fig. 1 - Block diagram of the detector system

The detector system is composed of :

1) an X-ray tube
2) a rotation and translation system
3) a point detector
4) an acquisition board
5) a 486 dx2 66 computer

The X-ray tube has an adjustable power supply from 15 to 110 KV with a maximum 3 mA current. Its beam is collimated before reaching the object thanks to a 10 mm hole in a 0.5 cm lead plate and after passing through the object thanks to a 350 μm pin-hole in a 2 mm lead plate. It was not possible to use smaller holes both because of collimation difficulties and because of the limited amount of energy reaching the detector.

The rotation-translation system is essentially composed of two step motors, one for rotation (equipped with a reduction gear) with a resolution of 0.15° and the other for translation with a resolution of 25 μm and a step precision of ±5μm. The two steppers are fed by a power card interfaced to the control system composed of the PC and the acquisition card.

The point detector is made up of a silicon photodiode (BPW34). The BPW34 is a P-I-N with an intrinsic layer of approximately 300μm. The efficiency of the detection device depends on incident energy and varies from 10% at 20 KeV down to 1% at 60 KeV. The purpose of the pin-hole above the detector is to decrease the active area and increase spatial resolution. The interaction of the X photons in the detector produces a charge of few fC's and it is thus necessary to amplify the signal using a highly sensitive but low-noise circuit. To this end a preamplifier having discrete components made up of two stages was constructed. The first stage is composed of a fet and an npn transistor in a cascode configuration and the second is composed of two transistors in an emitter follower configuration. The preamplifier outlet goes from the entry of a discriminator which compares the energy detected by a diode with a suitable reference threshold, chosen so as to eliminate noise. An impulse (TTL signal) appears at the discriminator outlet whenever the energy detected by the diode is above the reference threshold.

The acquisition card (a standard ISA card) is installed inside the PC and allows control of the handling system and the reading of the impulses coming out of the discriminator. This reading is synchronised with the feed frequency of the X-ray tube in such a way as to ensure that all detections relate to the same numbers of energy packets emitted by the source.

The computer contains software that allows control of the handling system (the rotation and translation setup), of the acquisition system (integration time of each reading) and a utility performing a pre-analysis of the readings acquired. Data are saved in a file and transferred to a workstation for processing and tomographic reconstruction.

CHARACTERISATION OF THE TOMOGRAPH

Characterisation of the tomograph consists of a series of measurements on well-defined samples for the purpose of measuring the performance of the system on the basis of user-chosen parameters [9, 10]. Noise, spatial resolution and contrast were then measured as a function of energy emitted by the X-ray tube and detection time.

Noise measurement

When a small region of a piece of constant thickness and homogeneous material, the signal, which in theory should not vary, oscillates around a mean value. The main causes of this are the following:

a) emissions from the source are not constant,
b) the behaviour of the detector, which is influenced by signal temperature and energy,
c) electronic system noise.

The system now allows modification of the energy emitted by the tube and variation of signal integration times. By providing for a second detector it would be possible to control energy emitted by the tube with time variations, thus irradiating it directly without going through the object: this would allow the *a posteriori* correction of the useful signal, which would be auspicable, especially with first-generation tomographs requiring very long detection times. Tests, conducted at air temperature on PVC samples of uniform thickness, were performed at 30, 45 and 70 KV, with detection times of 0.5, 1.0 and 2.0 seconds per point. The ratio between the standard deviation of the signal with respect to its mean value was measured: noise goes from 0.08% at 70 KV and 2.0 seconds integration time without the object to 2.3% at 30 KV and 0.5 seconds with a PVC sample 20 mm thick.

Spatial resolution and contrast

An important characteristic of a tomograph is its capacity to isolate small objects inside a volume. This is connected to both spatial resolution and contrast. As concerns the former, it is connected with beam size, acquisition step length and energy emitted by the tube. Medical tomographs today reach a spatial resolution on the order of 0.5 mm, and systems used in cases of osteoporosis are now capable of resolving to 90μm. As concerns industrial microtomographs, there are now systems capable of resolving to a few tenths of microns. To measure spatial resolution, the MTF (Modulation Transfert Function) was calculated on 20 mm thick PVC pieces, with variations in detection times and energy emitted by the tube. The translation step used was 50 μm. After acquiring the ERF (Edge Response Function, Fig. 2), a step signal caused by the passage from one thickness to another was filtered and derived to obtain the LSF (Line Spread Function, Fig. 3): The Fourier transform of this function leads to the MTF (Fig. 4) which measures the system's capacity to reveal quick variations in the signal and which is expressed in lines per millimetre. Analysis of results has shown that the value of MTF is 0.5 in correspondence to about 2.5 lines/mm and 0.1 for about 4 lines/mm. These values remain practically constant both with variations in energy emitted by the tube and with an increase in integration time. The factor that strongly limits system resolution is the poor collimation of the beam (a pin-hole of 350 μm). If we indicate the size of the source with the letter *a*, its distance from the object with the letter *q*, the diameter of the pin-hole in direct contact with the detector with the letter *d* and distance between source and pin-hole with the letter *L*, beam width (BW) is defined as the following quantity:

$$BW \cong \frac{\sqrt{d^2 + \left[a\left(M-1\right)\right]^2}}{M} \qquad \text{where} \qquad M = L/q$$

It can be demonstrated [9] that the smallest object the system is capable of identifying must be larger than BW/2 and that the contrast of objects smaller than BW will be less than the exact value. In our case d=350μm, M is close to unity and consequently the smallest object the system can reveal will be larger than 175μm.

As concerns contrast, Fig. 5 shows that it worsens with the increase in energy emitted by the tube, going from 67% at 30 KV to 25% at 70 KV. Conversely, signal integration time has no influence on contrast.

We also wished to verify the non-linear trend of X-ray attenuation with an increase in the thickness of the test piece object (beam hardening), a phenomenon connected with the polychromatic beam. A piece of PVC cut so as to present two thicknesses, 20 and 40 mm, was used. The passage through the smaller thickness reduces the detector count by 48% while passage through the second thickness, twice that of the former, reduces it by a further 36%. This is due to the fact that the first thickness stopped the lower energies and therefore mean beam energy increased. This result shows the necessity of working with monochromatic beams to supply the tomographic reconstruction algorithms with significant data and also shows how important it is to avoid test pieces whose cross sections are close to a greatly elongated rectangle.

The final test consisted of the tomography of a hollow PVC pipe 25 mm in diameter with a thickness of 4.0 mm. Four steel wires of different diameters, from 0.22 mm to 0.4 mm, and a 1.2 mm thick PVC sheath from which the copper wires had been removed, were placed inside the pipe. 560 linear data were acquired for 25 angles between 0° and 180° degrees: it took more than 4 hours to record the 14,000 data. To ensure that the tomography produces good results, it is of the utmost importance to know exactly the rotation centre of the handling system. This was overcome by acquiring the attenuation functions at 0° and 180°: the rotation centre represents the position of the axis allowing superimposition of the two recorded functions. For tomographic reconstruction we used the GH-MART algorithm, which required a calculation time of about two hours for 20 iterations on a Silicon Graphics R4400 workstation (175 Mhz, 32 Mb of RAM). In Figs. 6 and 7 some of the results are given. Fig. 8 shows the reconstruction with the classic filtered back-projection algorithm [5-6]: to obtain good results with this method many data are needed, and this leads to acquisition times that are impracticable for our system. On the other hand, calculation velocity and the memory requirements of this algorithm are decidedly better than in the case of algebraic techniques. The result of the tomography is quite significant: despite the noise present in the entire reconstructed section, it is possible to distinguish many small details, not last of which the hole inside the sheath, the size of which is no more than some tenths of a millimetre. The steel wires are quite evident since attenuation is proportional to the fourth power of the atomic number, which is about 12 for PVC and about 55.8 for steel.

Good agreement between the reconstructed image and the real object can be seen. The following table shows a comparison between the real dimensions of the test piece and those appearing in the tomographic reconstruction.

	real dimension (mm)	tomography (mm)
External diameter of PVC pipe	25.0	25.0 - 25.4
thickness	4.0	3.80 - 4.20
steel wire diameter	0.22 - 0.4	0.45 - 0.75
sheath diameter	1.2	1.0 - 1.4

These results confirm the theoretical analyses [9]. Noise on numerous homogeneous regions (each containing 100 pixels [9]), assumed values between 7% and 10% inside the cylinder; they are between 10% and 15%, with peaks around 20%, on the thickness.

To visualise results we developed algorithms capable of isolating characteristic surfaces inside the tomographically reconstructed volume or, alternatively, of visualising the entire volume with the volume rendering technique[13, 14].

CONCLUSIONS

Characterisation of the prototype of the X-ray microtomograph is still in progress. Up to now we have analysed PVC test pieces of suitable form and size for testing spatial resolution, contrast and noise and for finding the most effective energies and times. The low sensitivity level of the point detector caused quite long acquisition times which, to protect the X-ray tube, were limited. This led to a reduced number of data in the reconstruction stage. Results are such as to encourage development of the prototype: in particular, advances in acquisition systems will lead to a great improvement both in precision and acquisition times. In the near future, we expect to be able to use a new cooled sensor, about 80 times more sensitive than the one used previously, and this will mean an improvement in collimation and thus in system resolution.

Also expected in the future is the development of a third-generation tomograph in which a scintillator will convert the X-rays into green light visible to a cooled, high-resolution video camera and whose handling system will be limited to rotation only.

REFERENCES

[1] Kobayashi A.S. (Editor), Handbook of Experimental Mechanics, Prentice-Hall, Englewood Cliffs, NJ, pp.314-387, 1987.

[2] Summerscales J. (Editor), Non-destructive testing of fibre-reinforced plastics composites, Elsevier Applied Science, London and NewYork, 1990.

[3] Post D., Moiré Interferometry for Composites; Chap.IV, SEM Manual on Experimental Methods for Mechanical Testing of Composites, M.E.Tuttle and R.L.Pendleton, Editors, SEM, BETHEL, CT, 1989.

[4] Bertolino F., Ginesu F., Chen J., Experimental Characterization and Analysis of Angle-ply Composite Laminates, Proceedings of the 1994 SEM Spring Conference and Exhibits, 1994, Baltimore (Ma) pp.828-835.

[5] Rosenfeld A., Kak A.C., Digital Picture Processing, Computer Science and Applied Mathematics, Academic Press, 1982.

[6] Natterer F., The Mathematics of Computerized Tomography, John Wiley & Sons Ltd. and B.G.Teubner, Stuttgart, 1989.

[7] Bertolino F., Ginesu F., Savona V., Messa a punto di una tecnica di tomografia interferometrica, Atti del XXIV Convegno Nazionale AIAS, Parma, 1995.

[8] Snyder R., Hesselink L., High speed optical tomography for flow visualization, Applied Optics/Vol.24, No.23/pp.4046-4051, 1985.

[9] ASTM Guide E 1441-91: Standard Guide for Computed Tomography (CT) Imaging.

[10] Appoloni C.R., Cesareo R., Microscanning and microtomography with X-ray tubes, Centro interdipartimentale di ricerca per l'analisi dei modelli e dell'informazione nei sistemi biomedici, CISB, Univ. "La Sapienza" di Roma, Rap. 04.94, Dic. 1994.

[11] Gordon R., A Tutorial on ART (Algebraic Reconstruction Techniques), IEEE Transactions on Nuclear Science, Vol.NS-21, pp.78-93, June 1974.

[12] Verhoeven D., Multiplicative algebraic computed tomographic algorithms for the reconstruction of multidirectional interferometric data, Optical Engineering/ Vol.32 No.2, pp. 410-419, 1993.

[13] Kaufman A., Volume Visualization, IEEE Computer Society Press Tutorial, 1991.

[14] Bertolino F., Gatto G., Tecniche per la visualizzazione di immagini tomografiche, Seminario ADM Italo-Spagnolo, Napoli, 25-27 Luglio 1996.

CORRESPONDING AUTHORS:

F. Bertolino, G. Gatto, F. Ginesu
Department of Mechanical Engineering,
University of Cagliari
Piazza d'Armi, 09123 ITALY
E-MAIL: bertolin@iris.unica.it

P. Randaccio
Department of Physics
University of Cagliari
Via della Pineta, 09123 ITALY
E-MAIL: randaccio@vaxca.ca.infn.it

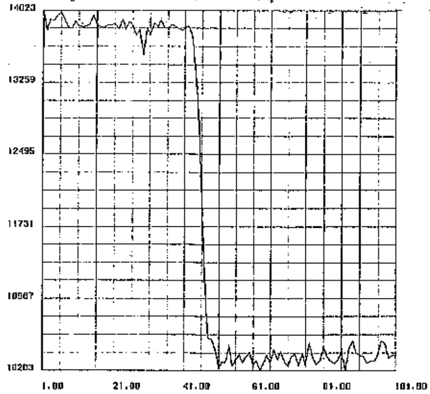

Fig. 2: Edge Response Function

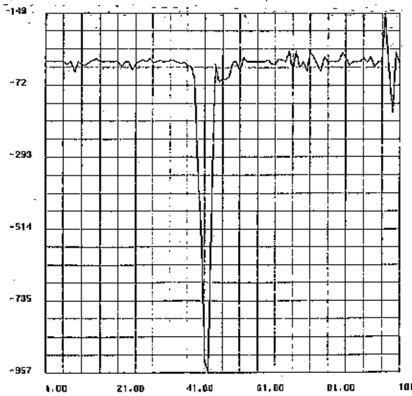

Fig. 3: Line Spread Function

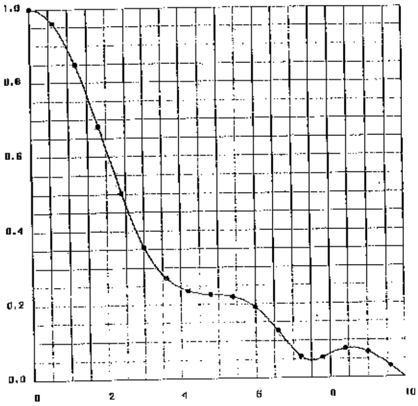

Fig. 4: Modulation Transfert Function

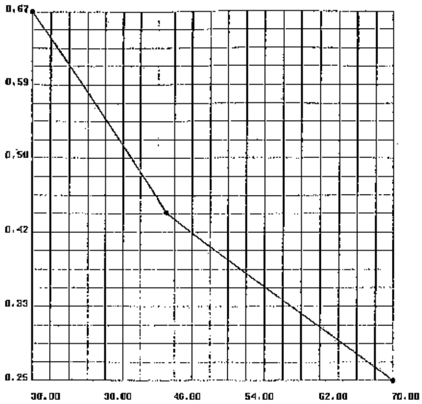

Fig.5: Contrast as a function of energy

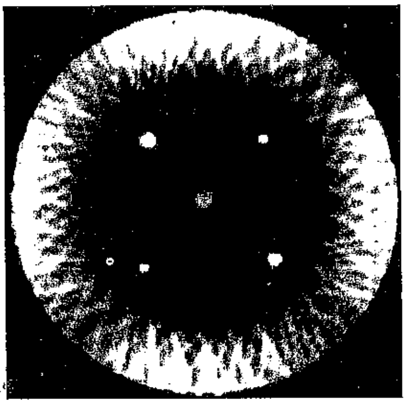

Fig. 6: Tomography of a cross section

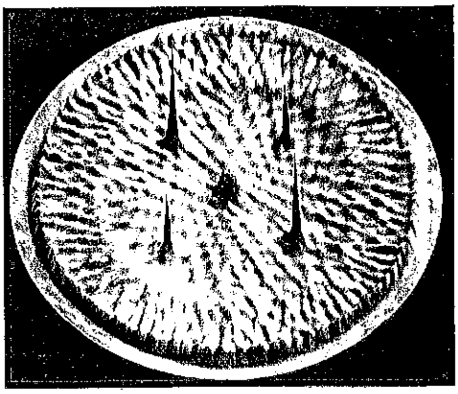

Fig. 7: X-ray attenuation function.

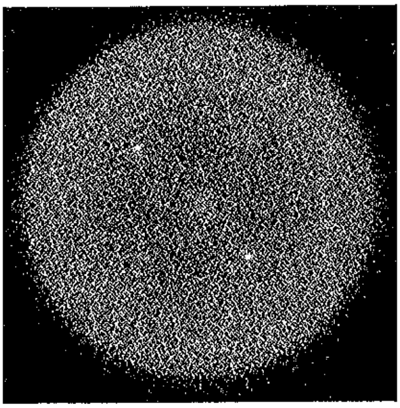

Fig. 8: Tomography of a cross section with the filtered back_projection algorithm